2586 *Chem. Mater.* **2009,** *21,* 2586–2588
DOI:10.1021/cm900623v

CHEMISTRY OF MATERIALS
Communication

Atomic Layer Deposition of Antimony Oxide and Antimony Sulfide

Ren Bin Yang,[†] Julien Bachmann,*[,†,‡] Manfred Reiche,[†] Jürgen W. Gerlach,[§] Ulrich Gösele,[†] and Kornelius Nielsch*[,‡]

[†]*Max Planck Institute of Microstructure Physics, Am Weinberg 2, D-06120 Halle, Germany,* [‡]*Institute of Applied Physics, Hamburg University, Jungiusstrasse 11, D-20355 Hamburg, Germany, and* [§]*Leibniz-Institute of Surface Modification, Permoserstrasse 15, D-04318 Leipzig, Germany*

Received March 4, 2009
Revised Manuscript Received May 14, 2009

To date, the literature has offered no method for the atomic layer deposition (ALD) of antimony chalcogenides.[1] ALD, however, offers several major advantages with respect to most other deposition techniques from the gas phase, in particular the possibility to deposit homogeneously onto complex materials (such as porous and fibrous ones), the typically low reaction temperatures (compatible with organic substrates), and the outstanding thickness control.[2] Thus the possibility to deposit antimony chalcogenides by ALD could expectedly benefit some of the applications of these materials.[3] To remedy the gap, we have explored the oxidative and acid–base chemistry of various antimony coordination compounds with small molecular weight. These investigations enable us to present below two ALD reactions based on tris(dimethylamido)antimony, $(Me_2N)_3Sb$, that yield high growth rates of Sb_2O_5 and Sb_2S_3 at 120 °C.[4]

The reactivity of the heavier group V elements is relatively inauspicious for ALD precursor chemistry. The Sb–C bond is not typically strong, which favors homolysis and thermal decomposition of the antimony alkyls (thermal decomposition being useful for CVD, but incompatible with ALD). Additionally, the lack of polarity of the Sb–C bond implies that antimony alkyls are quite inert to acids and bases. The alkoxides are hardly more reactive and tend to have lesser volatility. We found that amido-substituted stibines offer a good compromise between thermal stability, acid–base reactivity, and volatility. Tris(dimethylamido)antimony, $(Me_2N)_3Sb$, can react with both mild acids (H_2S) and strong oxidizers (O_3) to cleave the Sb–N bond cleanly.

When a reaction cycle consisting of consecutive exposures to $Sb(NMe_2)_3$ and O_3 is repeated 500 times at 120 °C on a flat Si substrate, a smooth, compact film is obtained, as observed by transmission electron microscopy (Figure 1). It is amorphous according to selected-area electron diffraction (inset). A root-mean-square surface roughness of 0.3 nm is evaluated by atomic force microscopy. The deposited thickness (quantified by spectroscopic ellipsometry) linearly depends on the number of ALD cycles performed, with a rate of approximately 1.85 Å/cycle (Figure 2). The growth rate remains constant over a wide window of precursor pulse and exposure durations (insets), which proves the self-limiting nature of the stepwise surface reaction (the hallmark of ALD growth). It varies moderately with substrate temperature between 120 and 270 °C (see Figure S1 in the Supporting Information), whereas thermal decomposition was observed beyond 300 °C.[5] Thus, we consider 120 and 270 °C as the approximate limits of the practical ALD window for this reaction.

*Corresponding author. E-mail: julien.bachmann@physik.uni-hamburg.de (J.B.); Kornelius.nielsch@physik.uni-hamburg.de (K.N.).

(1) Puurunen, R. L. *Appl. Phys. Rev.* **2005**, *97*, 121301. One exception: a concise report of a reaction yielding Sb_2O_5 with the impediments of caustic precursor and by-product and an elevated working temperature (500°C): Viirola, H.; Niinistö, L. *Thin Solid Films* **1994**, *251*, 127–135.
(2) (a) Knez, M.; Nielsch, K.; Niinistö, L. *Adv. Mater.* **2007**, *19*, 3425–3438. (b) Hyde, G. K.; Park, K. J.; Stewart, S. M.; Hinestroza, J. P.; Parsons, G. N. *Langmuir* **2007**, *23*, 9844–9849.
(3) The oxides are synergists for flame retardants, polymerization catalysts, and dopants for tin oxide (a–g); the sulfide is used in photonic crystals, solar cells, and solid-state lubrication (h–l); the selenide and telluride appear in phase-change memories and thermoelectrics (m–p): (a) Brebu, M.; Jakab, E.; Sakata, Y. *J. Anal. Appl. Pyrolysis* **2007**, *79*, 346–352. (b) Mostashari, S. M.; Baie, S. *J. Thermal Anal. Calorim.* **2008**, *94*, 97–101. (c) Zanetti, M.; Camino, G.; Canavese, D.; Morgan, A. B.; Lamelas, F. J.; Wilkie, C. A. *Chem. Mater.* **2002**, *14*, 189–193. (d) MacDonald, W. A. *Polym. Int.* **2002**, *51*, 923–930. (e) Minami, T. *Semicond. Sci. Technol.* **2005**, *20*, S35–S44. (f) Kleinjan, W. E.; Brokken-Zijp, J. C. M.; van de Belt, R.; Chen, Z.; de With, G. *J. Mater. Res.* **2008**, *23*, 869–880. (g) Huang, J.-L.; Pan, Y.; Chang, J. Y.; Yau, B.-S. *Surf. Coat. Technol.* **2004**, *184*, 188–193. (h) Juárez, B. H.; Rubio, S.; Sánchez-Dehesa, J.; López, C. *Adv. Mater.* **2002**, *14*, 1486–1490. (i) Khokhar, A. Z.; De La Rue, R. M.; Treble, B. M.; McComb, D. W.; Johnson, N. P. *Micro Nano Lett.* **2008**, *3*, 1–6. (j) Messina, S.; Nair, M. T. S.; Nair, P. K. *Thin Solid Films* **2007**, *515*, 5777–5782. (k) Rajpure, K. Y.; Bhosale, C. H. *Mater. Chem. Phys.* **2002**, *73*, 6–12. (l) Cho, M. H.; Ju, J.; Kim, S. J.; Jang, H. *Wear* **2006**, *260*, 855–860. (m) Meister, S.; Peng, H.; McIlwrath, K.; Jarausch, K.; Zhang, X. F.; Cui, Y. *Nano Lett.* **2006**, *6*, 1514–1517. (n) Lee, S.-H.; Jung, Y.; Agarwal, R. *Nat. Nanotechnol.* **2007**, *2*, 626–630. (o) Lee, J. S.; Brittman, S.; Yu, D.; Park, H. *J. Am. Chem. Soc.* **2008**, *130*, 6252–6258. (p) Martin-Gonzalez, M.; Prieto, A. L.; Gronsky, R.; Sands, T.; Stacy, A. M. *Adv. Mater.* **2003**, *15*, 1003–1006.

(4) **Experimental procedures.** Si wafers (100) and anodic alumina membranes (Whatman) were used as substrates. ALD was performed in a Cambridge Nanotech reactor with O_3 from an OzoneLabs generator and commercial precursors. ***Caution:*** *the precursors are volatile and toxic!* Pulse, expo, and purge times of ($Sb(NMe_2)_3$) are 1.4, 15, and 10 s for flat substrates; pulses are 0.2 and 0.1 s for O_3 and H_2S, respectively. Depositions on porous substrates require longer exposures and purges (30 s/20 s). A J. A. Woollam Co. M-44 variable angle spectroscopic ellipsometer was used to obtain thickness and optical constants of the films. The Cauchy and general oscillator models were applied to Sb_2O_5 and Sb_2S_3, respectively. An interfacial layer of 1.6 nm SiO_2 was included. Surface roughness was taken into account by an effective medium layer. TEM, EDX, and SAED were obtained on a Philips CM20-FEG at 200 kV. SEM was performed on a Jeol 6390. AFM was carried out on a Dimension 5000 from Digital. Negative-ion TOF-SIMS was performed with an ION-TOF instrument with 15 keV Ga^+ analysis source and 1 keV Cs^+ erosion source. Quantitative element analysis was carried out by atomic absorption at Kolbe Mikroanalytisches Laboratorium in Mühlheim, Germany.

(5) Yang, R. B.; Bachmann, J.; Pippel, E.; Berger, A.; Woltersdorf, J.; Gösele, U.; Nielsch, K. *Adv. Mater.* **2009**, 21, early view.

 Published on Web 05/29/2009 © 2009 American Chemical Society

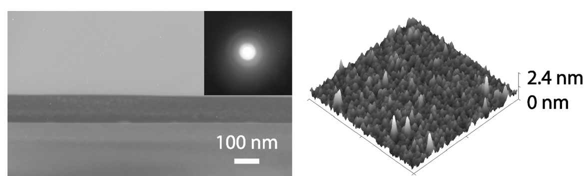

Figure 1. Morphology of an antimony oxide thin film deposited by ALD at 120 °C: Left, cross-sectional transmission electron micrograph (TEM) of the film (dark) on the Si substrate (below), with selected-area electron diffraction pattern (inset); right, atomic force micrograph (AFM) of the surface (1 μm × 1 μm).

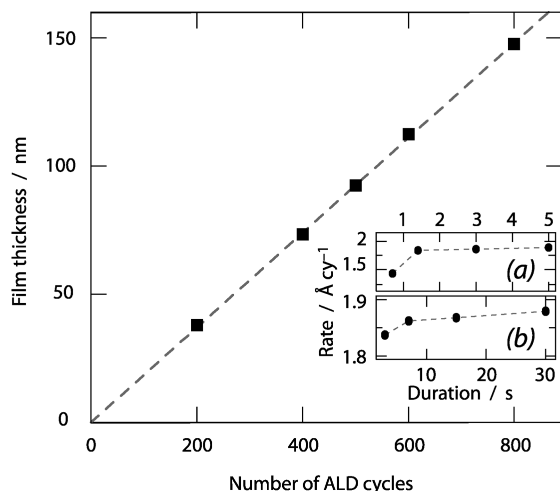

Figure 2. Linearity of the Sb_2O_5 film growth by ALD on a Si substrate at 120 °C, experimental data points (ellipsometry) with least-squares fit (R^2 > 0.999). Insets: growth rate dependence on the $Sb(NMe_2)_3$ pulse (a) and exposure durations (b), showing self-limiting behavior.

Energy-dispersive X-ray (EDX) spectroscopy of the films deposited by the ALD reaction between $Sb(NMe_2)_3$ and O_3 at 120 °C (Figure 3a) clearly shows the peaks of O and Sb, at the exclusion of other elements, consistent with the description of the solid as a pure antimony oxide. The quantification of oxygen by EDX being questionable, the method cannot reliably differentiate between Sb_2O_3 and Sb_2O_5. However, elemental analysis performed by atomic absorption delivers a Sb:O molar ratio of 28:72, consistent with the stoichiometry Sb_2O_5. A sputtered depth profile of the film obtained by mass spectrometry (TOF-SIMS, Figure 3b) further corroborates those data: the fragments SbO, O_2, Sb, and Sb_2O_3 figure among the most prominent. Signals appear for H, C, F, and NO with intensities an order of magnitude above those within the electronic-grade Si substrate. We tentatively attribute the significant Cl impurity to substrate preparation, because its intensity increases in the vicinity of the film/substrate interface.

The reaction of $Sb(NMe_2)_3$ with H_2S can also be performed in ALD mode, with significant differences with respect to the O_3 combustion. After exposure of Si wafers to consecutive pulses of the trisamidoantimony and hydrogen sulfide at 120 °C, thin but rougher films are obtained (Figure 4, root-mean-square surface roughness 1.6 nm). The roughness could either be an intrinsic consequence of the ALD reaction, or be due to oxidation of the surface upon exposure of the film to air. A growth

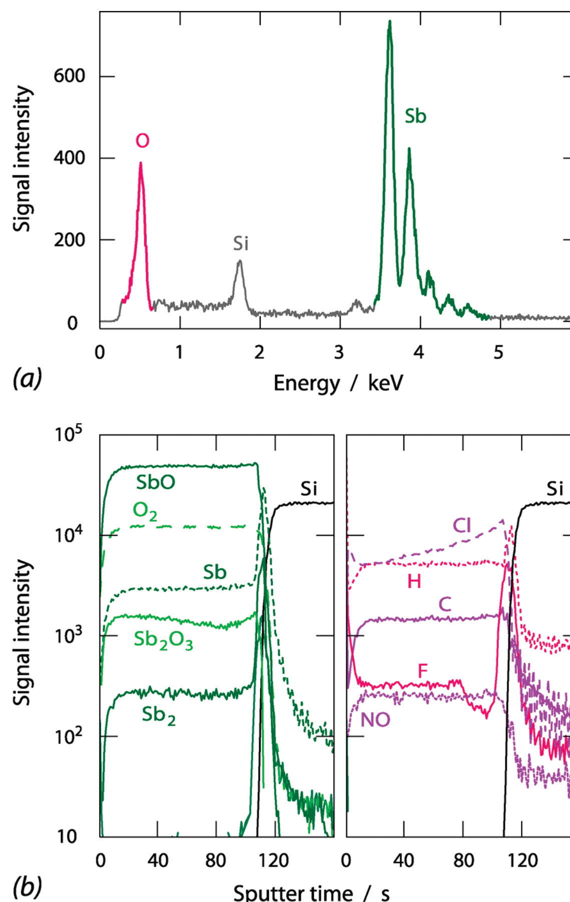

Figure 3. Chemical analyses of Sb_2O_5 films on silicon substrates. (a) Energy-dispersive X-ray spectrum (EDX; the Si signal originates from the substrate). (b) Mass spectrometric (TOF-SIMS) depth profile: the left panel shows the traces of the fragments originating from Sb_2O_5, the right panel contains signals due to impurities; in both, the Si signal shows the position of the interface between substrate and ALD film.

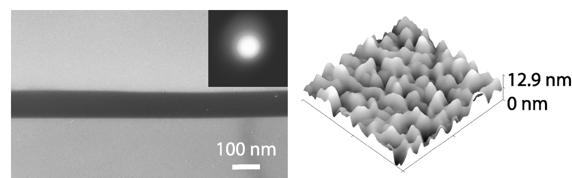

Figure 4. Morphology of an antimony sulfide thin film deposited by ALD: Left, cross-sectional transmission electron micrograph (TEM) of the film (dark) on the Si substrate (below), with selected-area electron diffraction pattern (inset); right, atomic force micrograph (AFM) of the surface (1 μm × 1 μm).

rate of 0.58 Å/cycle is measured by ellipsometry, without evidence of an incubation period (Figure S2 in the Supporting Information).[6] This points to a sufficient hydrolytic sensitivity of the amide toward hydroxyl groups at the native oxide surface of silicon. The ALD window is found at very low temperatures, from 65 to 120 °C (inset of Figure S2 in the Supporting Information).

The antimony sulfide films deposited by the ALD procedure are chemically very pure. The Sb:S ratio obtained by EDX (Figure 5a) is 39:61, which corresponds ideally to the stoichiometry Sb_2S_3. The presence of small C and O signals is related to the preparation of the

(6) A bias of about 10 nm is introduced, most likely as a measurement artifact by the surface roughness.

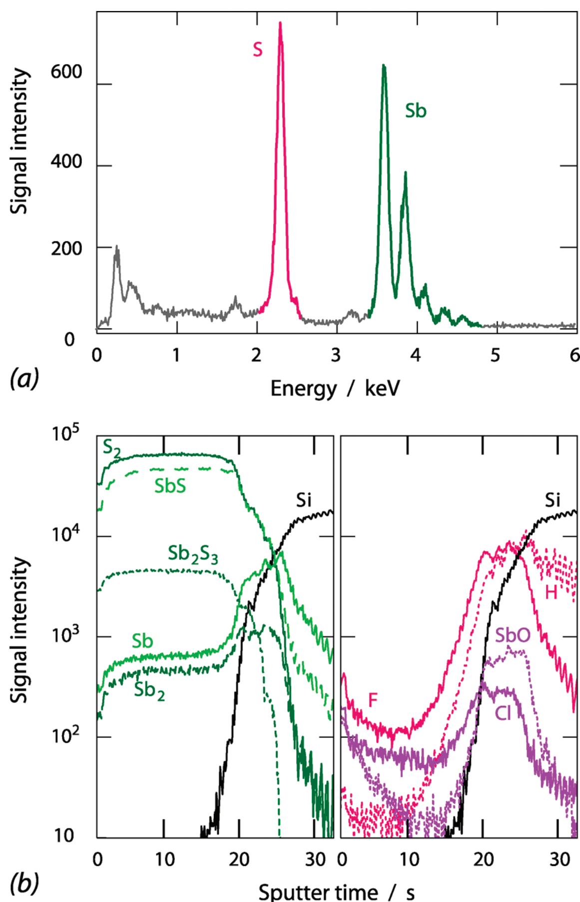

Figure 5. Chemical analyses of Sb_2S_3 films on silicon substrates. (a) Energy-dispersive X-ray spectrum (EDX). (b) Mass spectrometric (TOF-SIMS) depth profile: the left panel shows the traces of the fragments originating from Sb_2S_3, the right panel contains signals due to impurities; in both, the Si signal shows the position of the interface between substrate and ALD film.

ultrathin TEM sample. In the TOF-SIMS depth profile (Figure 5b), the only signals of significant intensities (more intense than in the Si substrate) belong to the fragments S_2, SbS, Sb, and Sb_2. In particular, contamination by C and H is extremely low. The higher purity obtained from the reaction of the amido stibine with H_2S than with O_3 can be interpreted as a consequence of the well-defined substitutional nature of the former reaction. The acid can only protonate at the N site, resulting in the specific heterolysis of the Sb–N bond and release of dimethylamine. In contrast to this, a combustion such as the one carried out with ozone is less selective and more likely to leave some poorly volatile products behind. The redox reaction with ozone also converts the Sb(+III) center in the molecular starting material to the oxidation state +V in Sb_2O_5. Conversely, the oxidation state of antimony is conserved in its reaction with the acid.

The optical properties of the films are accessible from the ellipsometric data. The refractive index (n) and extinction coefficient (k) spectra for the antimony oxide and antimony sulfide films grown at 120 °C are shown in Figure S3 in the Supporting Information. Sb_2O_5 is optically transparent in the visible, with a refractive index ranging from 1.85 at 1000 nm to 2.15 at 300 nm. In contrast to this, the reddish Sb_2S_3 films absorb significantly for $\lambda < 600$ nm, with a high refractive index between 2.9 and 3.6 over our spectral range, in agreement with reported values.[3i,7]

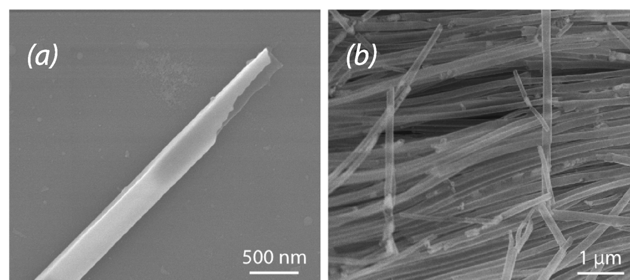

Figure 6. Scanning electron micrographs (SEM) of (a) Sb_2O_5 and (b) Sb_2S_3 nanotubes deposited by ALD in a porous alumina template at 120 °C, after dissolution of the matrix.

The ultimate proof of the self-limiting (that is, ALD) nature of the reactions is delivered by the ability of the processes to coat highly porous substrates with conformal films. Depositions of Sb_2O_5 and Sb_2S_3 into nanoporous anodic alumina membranes yield arrays of parallel nanotubes. Upon dissolution of the alumina matrix, the tubes can be observed in bundles under the scanning electron microscope (Figure 6). Temperature influences the formation of such nanostructures similarly to the films. For Sb_2O_5, a deposition temperature of 120 °C allows one to create tubes with aspect ratios in excess of 50, whereas depositions at 60 °C are limited to an aspect ratio of 8. In the case of Sb_2S_3, aspect ratios >100 are possible at both 65 and 120 °C.

Thus, the trisamido antimony precursor opens a breach into the quite hermetic realm of antimony chalcogenide ALD. It reacts both in oxidative conditions (with ozone) and in acid–base fashion (with hydrogen sulfide) to yield Sb_2O_5 and Sb_2S_3, with very favorable characteristics—low reaction temperature, high deposition rate, excellent material purity, high conformality. In the next steps, we plan on exploring the possiblities to access antimony selenide and telluride ALD using recently reported precursors for Se and Te.[8] Success in this endeavor would open the door to the application of ALD toward the preparation of various nanostructured V–VI materials, with exciting perspectives in particular for thermoelectric energy conversion.[9]

Acknowledgment. We thank T. Wagner and A. V. Szeghalmi for sharing their expertise in ellipsometry, S. Hopfe, E. Pippel, A. Berger, and J. Woltersdorf for their support with TEM, and M. Alexe for his help with AFM. R.B.Y. was funded by the International Max Planck Research School for Science and Technology of Nanostructures with a predoctoral fellowship. This work was supported by the German Ministry of Education and Research (BMBF, Contract 03X5519).

Supporting Information Available: Figures S1–S3 as mentioned in the text (PDF). This material is available free of charge via the Internet at http://pubs.acs.org.

(7) Tigau, N. *Cryst. Res. Technol.* **2007**, *42*, 281–285.
(8) Pore, V.; Hatanpää, T.; Ritala, M.; Leskelä, M. *J. Am. Chem. Soc.* **2009**, 3478–3480.
(9) Yang, R. G.; Chen, G.; Dresselhaus, M. S. *Nano Lett.* **2005**, *5*, 1111–1115.